AGU PUBLICATIONS

JGR

Journal of Geophysical Research: Atmospheres

RESEARCH ARTICLE

10.1002/2013JD020633

**Key Points:**

- Over Northeast Atlantic Ocean, half of clear areas lie within 5 km from clouds
- MODIS data show 50% higher aerosol optical thickness within 5 km from clouds
- Quality flags identify well ocean chlorophyll content data not biased by clouds

**Correspondence to:**
T. Várnai,
tamas.varnai@nasa.gov

**Citation:**
Várnai, T., and A. Marshak (2014), Near-cloud aerosol properties from the 1 km resolution MODIS ocean product, *J. Geophys. Res. Atmos.*, *119*, 1546–1554, doi:10.1002/2013JD020633.

Received 26 JUL 2013
Accepted 31 DEC 2013
Accepted article online 6 JAN 2014
Published online 15 FEB 2014

# Near-cloud aerosol properties from the 1 km resolution MODIS ocean product

**Tamás Várnai[1,2] and Alexander Marshak[2]**

[1]Joint Center for Earth System Technology, University of Maryland Baltimore County, Baltimore, Maryland, USA, [2]Climate and Radiation Laboratory, NASA Goddard Space Flight Center, Greenbelt, Maryland, USA

**Abstract** This study examines aerosol properties in the vicinity of clouds by analyzing high-resolution atmospheric correction parameters provided in the MODIS (Moderate Resolution Imaging Spectroradiometer) ocean color product. The study analyzes data from a 2 week long period of September in 10 years, covering a large area in the northeast Atlantic Ocean. The results indicate that on the one hand, the Quality Assessment (QA) flags of the ocean color product successfully eliminate cloud-related uncertainties in ocean parameters such as chlorophyll content, but on the other hand, using the flags introduces a sampling bias in atmospheric products such as aerosol optical thickness (AOT) and Angstrom exponent. Therefore, researchers need to select QA flags by balancing the risks of increased retrieval uncertainties and sampling biases. Using an optimal set of QA flags, the results reveal substantial increases in optical thickness near clouds—on average the increase is 50% for the roughly half of pixels within 5 km from clouds and is accompanied by a roughly matching increase in particle size. Theoretical simulations show that the 50% increase in 550 nm AOT changes instantaneous direct aerosol radiative forcing by up to 8 W/m$^2$ and that the radiative impact is significantly larger if observed near-cloud changes are attributed to aerosol particles as opposed to undetected cloud particles. These results underline that accounting for near-cloud areas and understanding the causes of near-cloud particle changes are critical for accurate calculations of direct aerosol radiative forcing.

## 1. Introduction

Over the years, numerous studies provided insights on atmospheric aerosols by analyzing satellite observations. In most cases the data analysis used satellite products developed specifically for atmospheric studies [e.g., *Hsu et al.*, 2004; *Diner et al.*, 2005; *Remer et al.*, 2005; *Torres et al.*, 2007]. Sometimes, however, these products can be complemented by aerosol information from atmospheric correction algorithms, whose primary goal is to remove atmospheric effects from measurements of surface properties [e.g., *Lyapustin et al.*, 2011, 2012]. For example, the atmospheric correction algorithm of the MODIS (Moderate Resolution Imaging Spectroradiometer) ocean color product [e.g., *Gordon and Wang*, 1994; *Wang and Shi*, 2007; *Ahmad et al.*, 2010] provides aerosol optical thickness (AOT) and Angstrom exponent (AE) data that offer several potential benefits.

First, the ocean product provides aerosol properties at a 1 km spatial resolution, which is higher than the 10 km resolution of the current, Collection 5 MODIS atmospheric aerosol product, or even higher than the 3 km resolution of the upcoming, Collection 6 product. The higher resolution can help study aerosols near discrete sources such as ships, volcanoes, and fires or industry near coastlines—and also to study aerosols near clouds. Second, the ocean algorithm uses an approach designed to minimize retrieval uncertainties caused by changes in sea conditions such as wind speed or algae content. Third, the ocean product includes carefully designed quality assurance (QA) parameters that can reveal the effect of various observation conditions on retrieved aerosol properties. While the MODIS atmospheric algorithm also provides QA parameters, the ocean product uses different methods to warn about factors such as the presence of absorbing aerosols, clouds, or sun glint that can affect the accuracy of the retrieval algorithm. Finally, ocean products provide atmospheric parameters even for some satellites that have no other aerosol products—for example, OCTS (Ocean Color and Temperature Scanner)—and this can increase the spatial/temporal coverage of a study.

This paper uses aerosol data from the MODIS ocean product to examine systematic differences between aerosol properties near clouds and far from clouds. Earlier studies revealed that aerosol scattering and particle size increase in a wide transition zone surrounding clouds [e.g., *Charlson et al.*, 2007; *Koren et al.*, 2007; *Su et al.*,

**Table 1.** List of the MODIS Ocean Product Quality Assessment (QA) Flags Discussed in This Study[a]

| QA flag | Description |
|---|---|
| absaer | Absorbing aerosol |
| chlwarn | Chlorophyll-A content product quality reduced |
| coastz | Failure in Chlorophyll-A content algorithm |
| coccolith | Coccolithopores detected |
| lowlw | Very low water-leaving radiance (cloud shadows) |
| modglint | Moderate sun glint contamination |
| prodfail | One or more parameters could not be computed |
| prodwarn | Questionable value for one or more parameters |
| sstwarn | Sea surface temperature quality reduced (e.g., cloud contamination) |
| straylight | Stray light contamination |

[a]More on each flag can be found at the introduction to atmospheric correction at http://oceancolor.gsfc.nasa.gov/DOCS/SeaDAS/seadas_training.html or at http://oceancolor.gsfc.nasa.gov/DOCS/Ocean_Level-2_Data_Products.pdf.

2008; *Tackett and Di Girolamo*, 2009; *Twohy et al*., 2009; *Várnai and Marshak*, 2011]. These studies discussed numerous processes that can contribute to the changes, including aerosols swelling in humid air, cloud processing of aerosols (for example, in-cloud aqueous oxidation and collision/coalescence), and the presence of undetected cloud particles [e.g., *Jeong and Li*, 2010]. The undetected cloud particles may occur, for example, in cloud fragments that have sheared off from adjacent clouds, in incipient or in decaying clouds, or in hesitant clouds that oscillate near saturation [e.g., *Koren et al*., 2009; *Bar-Or et al*., 2010]. Moreover, part of the observed aerosol behaviors likely comes from meteorological conditions (e.g., wind speed) being different in cloudy and clear regions. While MODIS data—both 10 km resolution aerosol products [e.g., *Loeb and Schuster*, 2008] and 1 km resolution solar reflectances [e.g., *Várnai and Marshak*, 2009]—proved very helpful in characterizing the transition zones surrounding clouds, the 1 km resolution aerosol data in the ocean product offers new opportunities in understanding the properties and radiative impacts of aerosols near clouds, as well as their differences from aerosols occurring far from clouds.

The outline of this paper is as follows. Section 2 describes the data set used in this study, while section 3 examines the importance of QA parameters in aerosol studies. Section 4 then discusses the radiative impact of near-cloud changes in aerosol properties. Finally, section 5 offers a brief summary.

## 2. Data

This paper analyzes a data set that contains data for a 2 week long period (14–29 September) in ten consecutive years (2002–2011). The analyzed data comes from a roughly 1000 km by 500 km region (45°–50°N, 5°–25° W) over the Atlantic Ocean that lies just southwest of the United Kingdom. (MODIS radiances from this area and time period were also analyzed in *Várnai and Marshak* [2009].) The data set is limited to viewing zenith angles less than 10° and has an average solar zenith angle of 48°.

The aerosol information comes from the R2012 version of the MODIS ocean color product, which provides at 1 km resolution the 869 nm aerosol optical thickness, the 443 nm–869 nm Angstrom exponent, and various QA flags (Table 1). For each 1 km pixel, the 550 nm aerosol optical thickness is estimated from the 869 nm optical thickness and Angstrom exponent values provided in the ocean color product.

The study examines the way aerosol properties depend on distance to the nearest low-level cloud. Following the earlier studies by *Wen et al*. [2007], *Su et al*. [2008], *Twohy et al*. [2009], and *Várnai and Marshak* [2009], we focus on low clouds because they are most likely to influence nearby aerosols, which are often concentrated at low altitudes. We identify low clouds using the 1 km resolution Collection 5 MODIS cloud mask (MYD35) if the 5 km resolution cloud top pressure product has a value exceeding 700 hPa, indicating a cloud top altitude below ~3 km.

## 3. Impact of QA Flags on Statistics

The operational MODIS ocean product includes a large number of QA flags. Validation studies have shown that MODIS ocean products agree well with independent measurements for pixels that are deemed reliable by all QA flags [e.g., *Bailey and Werdell*, 2006]. The importance of QA flags in the interpretation of ocean measurements is further illustrated in Figure 1. The figure shows that selecting only the best pixels (pixels where none of the QA flags give any warning) not only changes overall mean values but also yields a self-consistent data set in which the estimated Chlorophyll-A concentration is not sensitive to the proximity of clouds. In contrast, using all data would not only yield too high overall mean values (due mostly to pixels flagged by the *prodfail* QA parameter, which marks pixels where any of the Level 2 ocean parameter retrievals failed) but would also show a spurious decrease near clouds due to factors such as stray light contamination

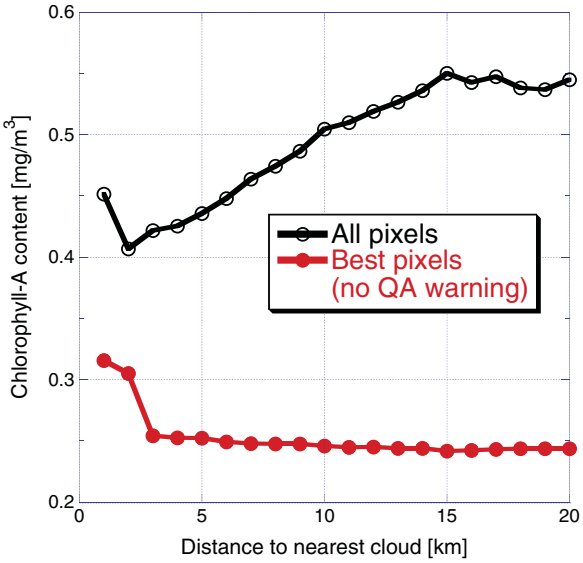


**Figure 1.** Mean retrieved Chlorophyll-A content when all data are used (black curve) and when only the best pixels are used (red curve).

[e.g., *Meister and McClain*, 2010], 3-D radiative processes [e.g., *Wen et al*., 2008], aerosol swelling [e.g., *Bar-Or et al*., 2012], cloud processing of aerosols [e.g., *Ervens et al*., 2011], and even the presence of undetected cloud particles [e.g., *Charlson et al*., 2007].

While the jump in Chlorophyll-A content within 2 km from clouds in Figure 1 indicates that QA parameters cannot filter out all pixels affected by these artifacts, the impact on large-scale ocean statistics is negligible. This is because the QA flags warn about potential artifacts near most clouds (Figure 2 inset shows that within 2 km from clouds, only a small fraction of pixels has no QA warning), and so only a small portion (<1%) of best pixels occurs within 2 km from clouds (Figure 2 red curve shows that the number of pixels without warning is much smaller near clouds than far from clouds). (Note that clouds have been identified using the MODIS cloud mask (MYD35) atmospheric product.) However, the figure also reveals that ensuring high quality greatly reduces the data volume. For ocean products, the reduction in data volume is usually not a critical concern, as ocean properties tend to change relatively slowly in time and space and even the reduced data amount can provide adequate sampling.

In contrast, using only the best pixels creates sampling issues for aerosol parameters, which vary on much shorter temporal and spatial scales. The sampling problems are especially important, because while the red curve in Figure 2 shows that only a small portion of best pixels lies near clouds, the black curve shows that most clear pixels are in fact close to clouds. Earlier studies have also found that due to systematic changes in atmospheric particles near clouds, excluding near-cloud pixels biases the results to underestimate aerosol radiative forcing. (*Twohy et al*. [2009] estimated "the aerosol direct radiative effect as derived from satellite observations of cloud-free oceans to be 35–65% larger than that inferred for large (>20 km) cloud-free ocean regions.") Therefore, researchers using aerosol data from the MODIS ocean product need to balance their competing needs for accurate retrievals and appropriate sampling. The optimal balance may be

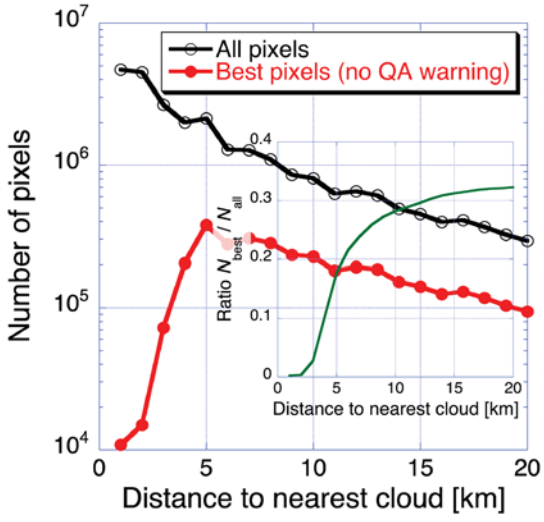


**Figure 2.** Number of pixels for two scenarios: (1) all data are used (black curve) and (2) only data without any QA warning are used (red curve). Inset: fraction of pixels that have no QA warning at all (best pixels).

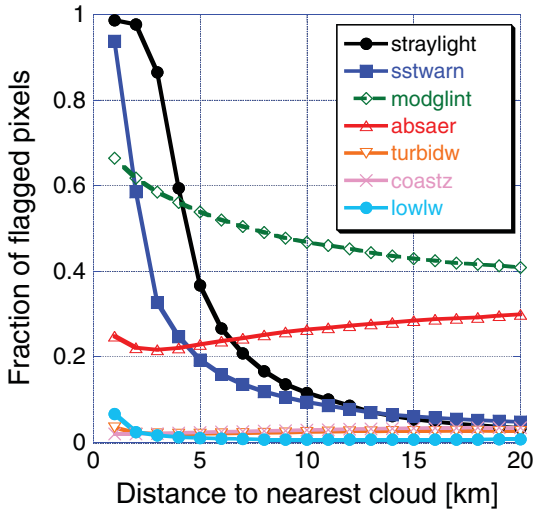


**Figure 3.** Fraction of pixels flagged by the most relevant QA flags: straylight (proximity of bright clouds and surfaces), sstwarn (cloud contamination), modlgint (sun glint), absaer (absorbing aerosol), turbidw (turbid water), coastz (coastal zone), and lowlw (cloud shadow). The fractions for a given distance bin do not add up to 1.0 because a single pixel can be flagged by several QA flags.

found by using a reduced set of QA flags to identify the pixels to be considered.

Figure 3 illustrates that most near-cloud warnings come from two cloud-related QA flags: *straylight* (which warns about stray light contamination by examining reflectance variations around a pixel) and *sstwarn* (which warns mostly about cloud contamination by examining patterns of near- and thermal infrared data). We note that a third cloud-related flag, *lowlw* (which warns about cloud shadows by checking whether a pixel appears too dark), affects much fewer pixels. The figure also shows that the frequency of occurrence changes with distance to clouds for two not inherently cloud-related QA flags: *modglint* (which warns about sun glint by checking spectral signatures), and *absaer* (which warns about the presence of absorbing aerosols by checking whether absorption makes visible reflectances much lower than expected from near-infrared data). At this point it is unclear why these parameters become more/less frequent near clouds, but it is entirely plausible that real changes cause this behavior. For example, wind—and hence glint properties—and the amount of absorbing aerosols may be different in weather patterns that favor clear skies. All other QA flags occur much less frequently, and so most of them are not even plotted in Figure 3.

Figure 4 illustrates the impact of some key QA flags on retrieved aerosol optical thickness. The black line is much higher than the other lines because it is based on all pixels, including even the ones that are flagged by the *modglint* flag. The presence of glint enhances the scene reflectance, and the retrieval algorithm erroneously attributes at least part of the enhancement to an increase in aerosol optical thickness. (In comparison, the impact of the *absaer* flag is much smaller.)

The comparison of the red curve—which uses all QA flags—with the orange, green, or blue curves—which use all flags except the *straylight* and/or *sstwarn* flags—shows that our perception of near-cloud AOT changes is greatly affected by whether we use or exclude pixels flagged by these two QA parameters. The orange line shows that the cloud contamination indicated by the *sstwarn* flag significantly increases optical thicknesses near clouds. The green line shows that the proximity to bright clouds (picked up by the *straylight* flag) causes even stronger increases in retrieved AOT. These increases may be attributed to several factors including stray light contamination, 3-D radiative processes, aerosol swelling, cloud processing of aerosols, and the presence of undetected cloud fragments (which are more frequent near detected clouds). We note that the increase in the blue curve is not equal to the sum of increases for the orange and green curves, because many pixels are flagged by both the *straylight* and *sstwarn* flags.

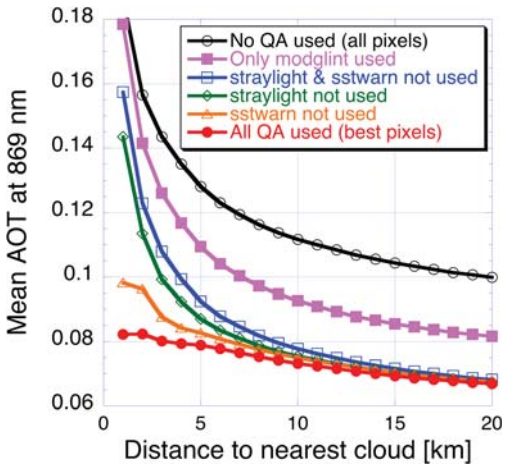


**Figure 4.** Near-cloud behavior of retrieved aerosol optical thickness if different sets of QA flags are used to filter the data. In the blue, green, and orange curves all QA flags are used except for the ones mentioned in the legend.

Finally, the red curve indicates that for the best pixels, the differences between AOT near and far from clouds are relatively small (23% between 1 and 20 km). This suggests that the QA flags are effective in filtering out most cloud-related features (artifacts).

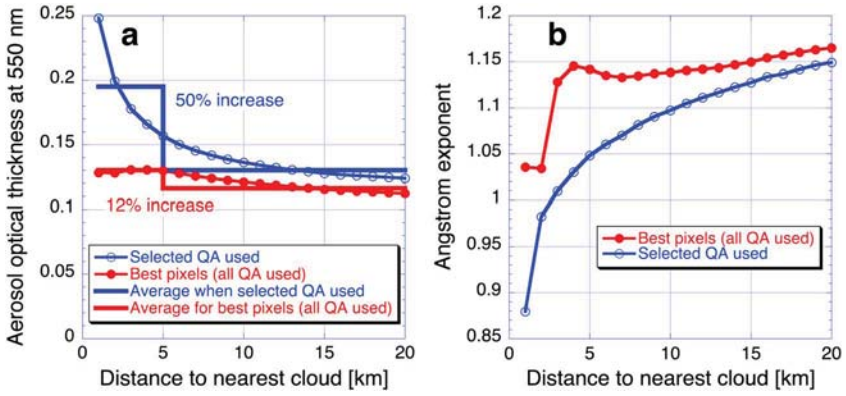


**Figure 5.** Near-cloud behavior of (a) 550 nm AOT (b) and 443–869 nm AE when using two different sets of QA flags. The red curves are obtained if all QA flags are used, while the blue curves are obtained when a selected set of QA flags is used. The 550 nm AOT is calculated from the 869 nm AOT and the AE reported in the MODIS ocean product. The thick lines in Figure 5a indicate the mean values weighted by the number of pixels at each distance, for two categories: areas closer than 5 km or farther than 5 km from the nearest cloud (including pixels farther than 20 km away). Approaching clouds from 20 km away to 1 km, the standard deviation of individual pixel values increases from 0.05 to 0.09 for AOT and from 0.34 to 0.41 for Angstrom exponent.

On the other hand, using all flags likely causes sampling biases by excluding large areas with strong AOT enhancements (e.g., near thick, bright clouds).

We can balance our concerns about artifacts (if no QA flags are used) and sampling biases (if all QA flags are used) by using a subset of all QA flags. For this, we use a subset that includes all QA flags except:

1. Three flags designed specifically for warning about the presence or proximity of clouds: *straylight*, *sstwarn*, *lowlw*. We do not use these flags because they would exclude the areas most affected by clouds. These areas are clearly essential for studying near-cloud behaviors of aerosol properties; moreover a large portion of clear sky is near clouds (e.g., Figure 2, or *Várnai and Marshak* [2012]).
2. Five flags that warn about problems specific to certain oceanic products: *prodfail*, *prodwarn*, *coastz*, *coccolith*, *chlwarn*. We do not use these flags for two reasons. First, these flags warn about problems that often come from limitations of the ocean retrieval algorithms. Second, because a much larger portion of satellite-observed signal comes from the atmosphere than from the ocean, aerosol retrievals are much less sensitive to slight inaccuracies than ocean retrievals. We note, however, that these flags are set much less frequently than the cloud-related flags, and so ignoring them does not significantly affect our aerosol statistics.

Figure 5 compares near-cloud changes in retrieved optical properties for the best pixels (not flagged by any QA flag) and for pixels not flagged by our subset of QA flags (which includes all QA flags except the eight mentioned above). (We note that if all QA flags except straylight and sstwarn are used, the results show similar behaviors to the blue lines.) As expected, the figure shows that near-cloud changes in both AOT at 550 nm and Angstrom exponent are substantially stronger if we use a subset of QA flags than if we use all flags. These changes and their radiative impacts are discussed in the next section.

## 4. Causes and Radiative Consequences of Near-Cloud Changes

As mentioned in the previous section, MODIS ocean products show significantly higher AOT and lower Angstrom exponent near clouds (Figure 5). These tendencies are consistent with earlier findings obtained for radiative quantities such as solar reflectances or lidar backscatters, color ratios, and depolarization ratios [e.g., *Koren et al*., 2007; *Su et al*., 2008; *Twohy et al*., 2009; *Várnai and Marshak*, 2009; *Yang et al*., 2012]. Analyzing the 1 km resolution MODIS ocean product offers new possibilities because the retrieved aerosol properties are easier to interpret and to put in perspective, and even to use in radiative calculations.

In order to avoid the sampling biases that underestimate near-cloud changes if we only use the best pixels not flagged by any QA flag, we focus on the results in Figure 5 that were obtained using a selected set of QA parameters (blue curves). Naturally, these results include some pixels affected by stray light contamination and 3-D radiative enhancements. The impact of these effects, however, is likely limited, for two reasons. First, *Várnai et al*. [2013] found strong stray light contamination only within 1 km from clouds. Second, the aerosol

retrievals rely greatly on long wavelengths where 3-D radiative effects are much weaker [e.g., *Wen et al*., 2008]: Aerosol properties are estimated by an iterative procedure that first estimates 869 nm AOT and 443–869 nm AE based on reflectances at 749 nm and 869 nm (where the ocean is very dark), and then refines these estimates using 443 nm reflectances, which help accounting even for the small ocean reflectance at the longer wavelengths [*Gordon and Wang*, 1994; *Wang and Shi*, 2007, and the introduction to atmospheric correction at http://oceancolor.gsfc.nasa.gov/DOCS/SeaDAS/seadas_training.html]. We note that 3-D effects, causing about a third of near-cloud increases in 550 nm reflectance in *Várnai et al*. [2013], may still impact the retrieval procedure through the 443 nm reflectance, but their magnitude is unclear at this point. Overall, we expect that the true values of optical thickness and AE are somewhere between the blue and red curves and are likely closer to the blue ones. We note, however, that retrieved optical properties characterize the entire particle population of an area, including undetected cloud particles, and so the results are likely affected by cloud contamination.

Figure 5a shows that near-cloud AOT changes are indeed substantial. For example, the thick blue line (showing the means weighted by pixel numbers for the 1–5 km and 6–20 km distances) shows that AOT is about 50% higher for the roughly half of areas that is within 5 km from the nearest cloud. We note that while the absolute value of changes is slightly larger at 550 nm than at 869 nm (e.g., blue curves in Figure 4 versus Figure 5a), the relative change is slightly larger at 869 nm because of a smaller background signal of surface reflection and Rayleigh scattering.

AE changes are perhaps not as intuitive, but one can put them in perspective using Mie calculations. For this, we performed some sample calculations using the size distributions of Models #3 and #6 (called "water soluble with humidity" and "wet sea salt type") in the MODIS atmospheric product over ocean [*Remer et al*., 2005] and using sulfate aerosol and sea salt refractive indices based on *D'Almeida et al*. [1991, Table 4.3]. (The MODIS model refractive indices are available only for the wavelengths used in the atmospheric product but not for 443 nm.) Subsequently, we increased particle radius by 15% through humidification using the approach in *Gassó et al*. [2000] and repeated the Mie calculations. We found that the simulations matched the observations best if we assumed a coarse mode fraction (in 550 nm AOT) of 16%, and assumed that in ¾ of the data set both fine and coarse modes swell equally near clouds (15% increase in radius), and in ¼ of the data set only the coarse mode particle number increases near clouds. In this case the overall mean 550 nm AOT increases by 42%, and the mean Angstrom exponent drops from 1.16 to 1.0—closely matching the changes between 20 km and 3 km distances from clouds in Figure 5 (43% increase in AOT, 0.15 drop in AE). While such initial simulation results cannot really distinguish between aerosol swelling and cloud contamination or cloud processing (that is, between changes only in size or both in size and number), future detailed calculations may well be able to make the distinction. Naturally, such detailed calculations will need to use same aerosol models as the retrievals, and will need to consider natural variability to reproduce changes not only in overall averages, but also within each scene (which may have different aerosol types or coarse mode fractions, etc.). We note that a few studies using satellite or ground-based data and simulations have already made important strides toward determining the contribution of various processes [e.g., *Tackett and Di Girolamo*, 2009; *Jeong and Li*, 2010; *Várnai and Marshak*, 2012].

Also, we note that some early indications suggest that the differences between near-cloud and far-from-cloud particles come partly from local gradients within cloudy scenes and partly from differences between large-scale meteorological conditions (e.g., wind speed and air mass origins) in cloudy and clear areas. This issue will be explored in detail in a separate study that is now in its early stages.

Finally—unlike solar reflectances or lidar backscatter—the particle properties in Figure 5 allow one to examine the radiative impact of near-cloud changes. As an initial step to roughly gauge the radiative impact of near-cloud changes, we performed several calculations using the Coupled Ocean and Atmosphere Radiative Transfer model [*Jin et al*., 2006]. The calculations used 48° solar zenith angle, 6 m/s wind speed, 2 km water depth, 0.2 mg/m$^3$ chlorophyll content, and a midlatitude summer atmosphere with the MODerate resolution atmospheric TRANsmission (MODTRAN) maritime aerosol model. The results in Figure 6 show that if AOT increases from 0.130 (mean for the half of clear-sky areas that lie farther than 5 km from clouds) to 0.195 (mean for the half of clear-sky areas that are within 5 km from clouds) while other aerosol parameters remain unchanged, the reflected broadband flux increases by 6.4 W/m$^2$ (from 87.16 to 93.53 W/m$^2$), while the downwelling flux at the surface decreases by 8 W/m$^2$ (from 660.2 to 652.2 W/m$^2$). If the near-cloud changes are attributed not to

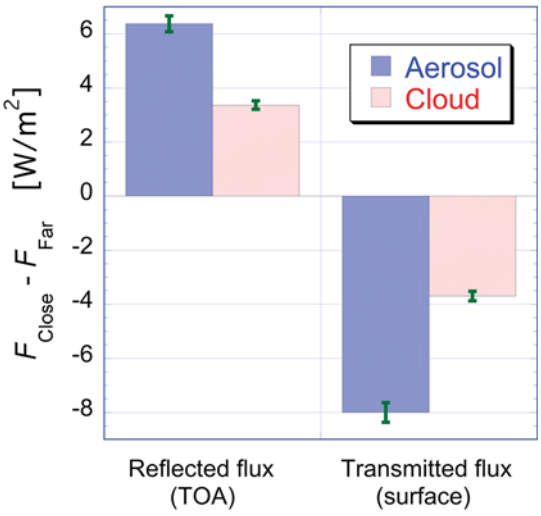


**Figure 6.** Impact of optical thickness differences between areas closer and farther than 5 km from clouds on instantaneous direct radiative forcing. Solid blue and red striped bars show the impact for two interpretations of Figure 5a: all observed optical thickness changes are attributed to aerosols (blue) and to undetected clouds (red). Error bars show uncertainties due to annual variability over the 10 years period used.

aerosols but to undetected cloud particles (having an effective radius of 15 μm and occurring between 1 km and 2 km altitudes), the increase in top-of-atmosphere (TOA) reflected shortwave flux is 3.4 W/m$^2$ and the decrease in downwelling flux at the surface is 3.7 W/m$^2$. Finally, if we assume that the difference between areas within and outside 5 km from clouds does not have a daily cycle, we can also estimate its impact on 24 h average fluxes. For the period of observations (second half of September), the estimated flux differences are 2.7 W/m$^2$ (TOA up) and 3.7 W/m$^2$ (surface down) if attributed to aerosols, and 1.6 W/m$^2$ (TOA up) and 2.1 W/m$^2$ (surface down) if attributed to undetected clouds.

These results have two important implications. First, they show that near-cloud changes in particle populations have a substantial radiative effect regardless of the exact mechanism causing the changes. Second, they show that it is important to find out the cause of near-cloud changes, because while the impacts are large in any case, they can be significantly different if they are caused by swollen aerosol particles or by undetected cloud droplets.

We expect that finding out the cause of near-cloud changes in particle properties, combined with future analysis along the line of *Várnai et al.* [2013], will provide a complete accounting for observed near-cloud changes in radiative and microphysical properties. We note that *Várnai et al.* [2013] combined MODIS global data analysis with theoretical simulations and found that roughly two thirds of near-cloud changes in 0.55 μm MODIS reflectances were caused by particle changes, much of the rest were caused by 3-D radiative effects, but instrument effects were important only within a km or so from clouds.

## 5. Summary

This paper uses satellite data to examine the systematic differences between near-cloud and far-from-cloud aerosols over the northeast Atlantic Ocean. In particular, it analyzes atmospheric correction data—aerosol optical thickness and Angstrom exponent—provided in the MODIS ocean color product. This data offers important benefits for atmospheric studies, because aerosol parameters are estimated using an approach that minimizes retrieval uncertainties caused by variations in sea conditions, retrievals are provided at a high (1 km) spatial resolution, and the retrieved aerosol parameters are accompanied by carefully designed quality assessment (QA) parameters. We note that aerosol information is available even in the ocean color product of some satellites lacking designated atmospheric products (e.g., OCTS).

By analyzing data from the second half of September over a 10 year long period, the study finds that the appropriate use of the QA flags for data selection is indeed essential. The results show that in studies of ocean parameters such as chlorophyll content, using all QA flags can successfully eliminate cloud-related problems and provide unbiased sampling. In studies of aerosol parameters, however, researchers need to carefully select the QA parameters they use. In this selection they need to balance higher retrieval uncertainties at pixels flagged by cloud-related QA parameters against dramatically reduced and potentially biased sampling if these pixels are not used.

In obtaining comprehensive statistics and examining near-cloud behaviors, this study uses a limited set of QA parameters and considers even the pixels flagged by cloud-related QA parameters, most importantly the *straylight* and *sstwarn* flags. The results reveal that optical thickness differs drastically near and far from clouds —on average, it is 50% higher for the roughly half of pixels within 5 km from clouds than for the half of pixels

that is more than 5 km away from clouds. At the same time, retrieved Angstrom exponents decrease near clouds, suggesting an increase in particle size that is roughly compatible with the optical thickness increase.

Broadband radiative calculations indicate that these changes affect instantaneous average aerosol radiative forcing by up to 8 W/m$^2$. The calculations also reveal that while the radiative impact is large in any case, it is much larger if near-cloud changes are caused by aerosol particles rather than by undetected cloud droplets.

Overall, the results underline that considering near-cloud areas and understanding the causes of near-cloud particle changes are critical for accurate calculations of direct aerosol radiative forcing. Finally, we note that understanding near-cloud behaviors is also important for accurate characterizations of aerosol-cloud interactions and indirect aerosol radiative forcing.

**Acknowledgments**
We gratefully acknowledge support for this research by the NASA Radiation Sciences Program managed by Hal Maring and by the NASA CALIPSO project supervised by Charles Trepte as the technical officer. We also thank Ziauddin Ahmad, Bryan Franz, Gerhard Meister, and other members of the MODIS ocean color team, as well as Bob Charlson, Guoyong Wen, Rob Wood, and Weidong Yang for insightful discussions and help.

## References

Ahmad, Z., B. A. Franz, C. R. McClain, E. J. Kwiatkowska, J. Werdell, E. P. Shettle, and B. N. Holben (2010), New aerosol models for the retrieval of aerosol optical thickness and normalized water-leaving radiances from the SeaWiFS and MODIS sensors over coastal regions and open oceans, *Appl. Opt.*, *49*, 5545–5560.

Bailey, S. W., and P. J. Werdell (2006), A multi-sensor approach for the on-orbit validation of ocean color satellite data products, *Remote Sens. Environ.*, *102*, 12–23, doi:10.1016/j.rse.2006.01.015.

Bar-Or, R. Z., I. Koren, and O. Altaratz (2010), Estimating cloud field coverage using morphological analysis, *Environ. Res. Lett.*, *5*, doi:10.1088/1748-9326/5/1/014022.

Bar-Or, R. Z., I. Koren, O. Altaratz, and E. Fredj (2012), Radiative properties of humidified aerosols in cloudy environment, *Atmos. Res.*, *118*, 280–294.

Charlson, R., A. Ackerman, F. Bender, T. Anderson, and Z. Liu (2007), On the climate forcing consequences of the albedo continuum between cloudy and clear air, *Tellus*, *59*, 715–727.

Diner, D., J. V. Martonchik, R. A. Kahn, B. Pinty, N. Gobron, D. L. Nelson, and B. N. Holben (2005), Using angular and spectral shape similarity constraints to improve MISR aerosol and surface retrievals over land, *Remote Sens. Environ.*, *94*, 155–171.

Ervens, B., B. J. Turpin, and R. J. Weber (2011), Secondary organic aerosol formation in cloud droplets and aqueous particles (aqSOA): A review of laboratory, field and model studies, *Atmos. Chem. Phys.*, *11*, 11,069–11,102, doi:10.5194/acp-11-11069-2011.

Gassó, S., et al. (2000), Influence of humidity on the aerosol scattering coefficient and its effect on the upwelling radiance during ACE-2, *Tellus B*, *52*, 546–567, doi:10.1034/j.1600-0889.2000.00055.x.

Gordon, H. R., and M. Wang (1994), Retrieval of water-leaving radiance and aerosol optical thickness over the oceans with SeaWiFS: A preliminary algorithm, *Appl. Opt.*, *33*, 443–452.

Hsu, N. C., S. C. Tsay, M. D. King, and J. R. Herman (2004), Aerosol properties over bright-reflecting source regions, *IEEE Trans. Geosci. Remote Sens.*, *42*, 557–569.

Jeong, M.-J., and Z. Li (2010), Separating real and apparent effects of cloud, humidity, and dynamics on aerosol optical thickness near clouds, *J. Geophys. Res.*, *115*, D00K32, doi:10.1029/2009JD013547.

Jin, Z., T. P. Charlock, K. Rutledge, K. Stamnes, and Y. Wang (2006), Analytical solution of radiative transfer in the coupled atmosphere–ocean system with a rough surface, *Appl. Opt.*, *45*, 7443–7455, doi:10.1364/AO.45.007443.

Koren, I., L. A. Remer, Y. J. Kaufman, Y. Rudich, and J. V. Martins (2007), On the twilight zone between clouds and aerosols, *Geophys. Res. Lett.*, *34*, L08805, doi:10.1029/2007GL029253.

Koren, I., G. Feingold, H. Jiang, and O. Altaratz (2009), Aerosol effects on the inter-cloud region of a small cumulus cloud field, *Geophys. Res. Lett.*, *36*, L14805, doi:10.1029/2009GL037424.

Loeb, N. G., and G. L. Schuster (2008), An observational study of the relationship between cloud, aerosol and meteorology in broken low-level cloud conditions, *J. Geophys. Res.*, *113*, D14214, doi:10.1029/2007JD009763.

Lyapustin, A., Y. Wang, I. László, R. Kahn, S. Korkin, L. Remer, R. Levy, and J. Reid (2011), Multi-angle implementation of atmospheric correction (MAIAC): Part 2. Aerosol algorithm, *J. Geophys. Res.*, *116*, D03211, doi:10.1029/2010JD014986.

Lyapustin, A., Y. Wang, I. Laszlo, T. Hilker, F. Hall, P. Sellers, J. Tucker, and S. V. Korkin (2012), Multi-angle implementation of atmospheric correction for MODIS (MAIAC), Part 3: Atmospheric correction, *Remote Sens. Environ.*, *127*, 385–393, doi:10.1016/j.rse.2012.09.002.

Meister, G., and C. R. McClain (2010), Point-spread function of the ocean color bands of the Moderate Resolution Imaging Spectroradiometer on Aqua, *Appl. Opt.*, *49*, 6276–6285.

Remer, L. A., et al. (2005), The MODIS aerosol algorithm, products, and validation, *J. Atmos. Sci.*, *62*, 947–973.

Su, W., G. L. Schuster, N. G. Loeb, R. R. Rogers, R. A. Ferrare, C. A. Hostetler, J. W. Hair, and M. D. Obland (2008), Aerosol and cloud interaction observed from high spectral resolution lidar data, *J. Geophys. Res.*, *113*, D24202, doi:10.1029/2008JD010588.

Tackett, J. L., and L. Di Girolamo (2009), Enhanced aerosol backscatter adjacent to tropical trade wind clouds revealed by satellite-based lidar, *Geophys. Res. Lett.*, *36*, L14804, doi:10.1029/2009GL039264.

Torres, O., A. Tanskanen, B. Veihelmann, C. Ahn, R. Braak, P. K. Bhartia, P. Veefkind, and P. Levelt (2007), Aerosols and surface UV products from Ozone Monitoring Instrument observations: An overview, *J. Geophys. Res.*, *112*, D24S47, doi:10.1029/2007JD008809.

Twohy, C. H., J. A. Coakley Jr., and W. R. Tahnk (2009), Effect of changes in relative humidity on aerosol scattering near clouds, *J. Geophys. Res.*, *114*, D05205, doi:10.1029/2008JD010991.

Várnai, T., and A. Marshak (2009), MODIS observations of enhanced clear sky reflectance near clouds, *Geophys. Res. Lett.*, *36*, L06807, doi:10.1029/2008GL037089.

Várnai, T., and A. Marshak (2011), Global CALIPSO observations of aerosol changes near clouds, *Geosci. Remote Sens. Lett.*, *8*, 19–23.

Várnai, T., and A. Marshak (2012), Analysis of co-located MODIS and CALIPSO observations near clouds, *Atmos. Meas. Tech.*, *5*, 389–396.

Várnai, T., A. Marshak, and W. Yang (2013), Multi-satellite aerosol observations in the vicinity of clouds, *Atmos. Chem. Phys.*, *13*, 3899–3908, doi:10.5194/acp-13-3899-2013.

Wang, M., and W. Shi (2007), The NIR-SWIR combined atmospheric correction approach for MODIS ocean color data processing, *Opt. Express*, *15*, 15,722–15,733.

Wen, G., A. Marshak, R. F. Cahalan, L. A. Remer, and R. G. Kleidman (2007), 3-D aerosol-cloud radiative interaction observed in collocated MODIS and ASTER images of cumulus cloud fields, *J. Geophys. Res.*, *112*, D13204, doi:10.1029/2006JD008267.

Wen, G., A. Marshak, and R. F. Cahalan (2008), Importance of molecular Rayleigh scattering in the enhancement of clear sky radiance in the vicinity of boundary layer cumulus clouds, *J. Geophys. Res.*, *113*, D24207, doi:10.1029/2008JD010592.

Yang, W., A. Marshak, T. Várnai, O. V. Kalashnikova, and A. B. Kostinski (2012), CALIPSO observations of transatlantic dust: Vertical stratification and effect of clouds, *Atmos. Chem. Phys.*, *12*, 11,339–11,354, doi:10.5194/acp-12-11339-2012.